

UC Berkeley

UC Berkeley Previously Published Works

Title

The Expression Pattern of Systemically Injected AAV9 in the Developing Mouse Retina Is Determined by Age

Permalink

<https://escholarship.org/uc/item/820674rn>

Journal

Molecular Therapy, 23(2)

ISSN

1525-0016

Authors

Byrne, Leah C
Lin, Yvonne J
Lee, Trevor
et al.

Publication Date

2015-02-01

DOI

10.1038/mt.2014.181

Peer reviewed

The Expression Pattern of Systemically Injected AAV9 in the Developing Mouse Retina Is Determined by Age

Leah C Byrne^{1,2}, Yvonne J Lin¹, Trevor Lee¹, David V Schaffer^{1,2} and John G Flannery¹

¹Helen Wills Neuroscience Institute, University of California Berkeley, Berkeley, California, USA; ²Department of Chemical Engineering and Department of Bioengineering, University of California, Berkeley, California, USA

Systemic delivery of AAV9 offers the potential for widespread and efficient gene delivery to the retina, and may thus be a useful approach for treatment of disease where intraocular injections are not possible, for syndromes affecting multiple organs, or where early intervention is required. The expression resulting from intravenous injection of AAV9 is more efficient in neonates than adults, and here we characterize the effect of age on retinal transduction of AAV9 in the mouse retina. We find that the pattern of expression in neonatal mice is correlated to the development of the retinal vasculature, and that the area of the retinal transduction as well as the cell types infected vary depending on the age at injection. Furthermore, we demonstrate that sequential injections of AAV9 vectors carrying two different transgenes infect adjacent areas of the retina, providing a larger area of coverage. Lastly, we show that the retina's endogenous spatiotemporal expression pattern of *Mfsd2a*, a protein associated with the maturation of a functional blood–brain barrier, coincides with suppression of retinal transduction by intravenously-delivered AAV9, suggesting that AAV9 crosses the blood–retina barrier through transcytosis.

Received 17 July 2014; accepted 9 September 2014; advance online publication 14 October 2014. doi:10.1038/mt.2014.181

INTRODUCTION

The recent discovery that adeno-associated virus serotype 9 (AAV9) has the ability to cross the blood–retina barrier raised the possibility of widespread gene delivery to the eye via a noninvasive approach.^{1–3} Although substantial hurdles exist for systemic gene delivery in the eye, intravenous injections offer the potential for bilateral gene delivery to a wide area of the retina, especially in cases such as glaucoma or retinoblastoma where intraocular injections are not suitable. Furthermore, systemic injections may even allow for prenatal or neonatal gene delivery at the earliest stages of retinal disease progression, leading to more efficient phenotypic rescue.

Systemic delivery of AAV9 to the retina has been analyzed in a number of rodent and large animal models, including mouse,^{1–3} rat, cat, dog,⁴ and primate.⁵ In each of these species, systemic injection of AAV9 vectors carrying GFP led to transgene expression in the eye. Additionally, tyrosine-to-phenylalanine mutations, which protect vector particles from proteasome degradation,⁶ increase

retinal transduction of AAV9³. Interestingly, age specific effects from systemic injections have been noted. In particular, while prenatal and neonatal administration of AAV9 leads to widespread transduction of the nervous system, maturation of the blood–brain barrier limits the reach of the vector.

In mice, an important model of retinal degenerative disease, Bostick *et al.* reported efficient gene transfer to the inner retina of neonatal, but not adult mice. Within the murine retina, the vasculature of the inner retina develops after birth, undergoing dramatic expansion and increasing in complexity during the first week,⁷ a process that is analogous to the expansion of human retinal vasculature *in utero*.⁸ During this process, the blood–retina barrier also forms and matures. Here, we characterize the transduction profile of AAV9 from 1 to 9 days after birth and show that the pattern of retinal vasculature development directly impacts the pattern of retinal gene expression, while in contrast brain expression remains constant. Furthermore, we show that two different vectors can be injected sequentially via the murine tail vein to mediate delivery of two distinct transgenes to adjacent regions, collectively leading to widespread coverage of the retina. Finally, we investigate retinal blood vessel development and demonstrate that *Mfsd2a*—a factor associated with blood–brain barrier maturation—is lacking at the leading edge of retinal vasculature during development, corresponding to the area of retinal transduction.

RESULTS

The pattern of AAV9 vector expression in the retina is altered by age at injection

To test the effect of organismal age on the pattern of retinal transgene expression, neonatal mice were systemically injected 1, 3, 5, 7, or 9 days after birth with 5×10^{11} – 1×10^{12} viral particles of AAV9 Y446E, Y731F (AAV92YF)-GFP (Figure 1). Groups of 5–7 mice were injected for each time point tested. The pattern of GFP expression in the retina at all time points closely matched the area corresponding to the leading edge of blood vessel growth⁷ at the day of injection. Injections at P1 yielded GFP expression that was limited to the central retina, surrounding the optic nerve head (ONH). P3 injections resulted in an expanded area of expression, with a void in GFP expression in the central retina at the ONH. Injections at P5 led to expression approximately 2/3 of the distance to the periphery of the retina, with an even larger expanding area lacking expression in the central retina. P7 injections led to transduction at the far periphery

Correspondence: Leah C Byrne, Helen Wills Neuroscience Institute, University of California Berkeley, 278 Stanley Hall, Berkeley, California 94720, USA. E-mail: lbyrne@berkeley.edu

of the retina, resulting in a wide ring of GFP expression. Finally, injections at P9 resulted in low levels of GFP expression in isolated cells observed across the retina.

Higher resolution images of retinal whole mounts revealed a more detailed view of GFP expression following systemic injection at P1, P5, and P9 (Figure 2). Imaging confirmed that injections at P1 led to GFP expression in cell bodies near the ONH, but no expression in the periphery. In contrast, P5 injections led

to GFP expression in cells approaching the peripheral edge of the retina, and expression was also visible in ganglion cell axons traveling to the ONH (arrowhead), but in fewer cell bodies near the ONH. P9 injections transduced a sparse population of cells across the retina. Finally, retinal pigment epithelium (RPE) flatmounts showed that P1 and P5 injections led to GFP expression in RPE cells across the retina, while fewer cells were transduced with injections at P9.

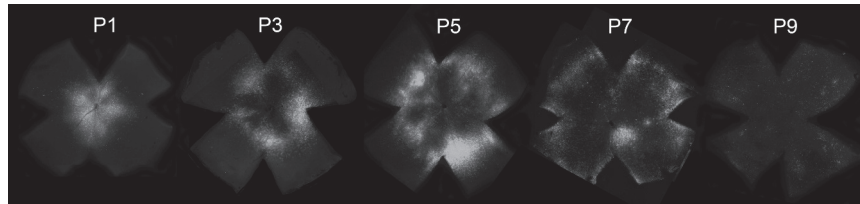


Figure 1 The expression pattern of systemically injected AAV9 in the retina was determined by age at injection. Tail vein injections of AAV9-scCAG-GFP (5×10^{11} DNase-resistant viral particles in a 10 μ l volume for mice aged P1–P5, and 1×10^{12} DNase-resistant viral particles in a 20 μ l volume for mice aged P7–P9) resulted in GFP expression in the retina. Retinal whole mounts from mice injected at increasing ages showed a changing expression pattern of GFP, correlating with the developmental pattern of the retinal vasculature. In mice injected at P1, expression was limited to a central region surrounding the optic nerve head. In mice injected at older ages, GFP was expressed at the leading edge of the developing retinal blood vessels, with an increasingly large area lacking expression in the center of the retina. In mice injected at P9, GFP expression in the retina is sparse.

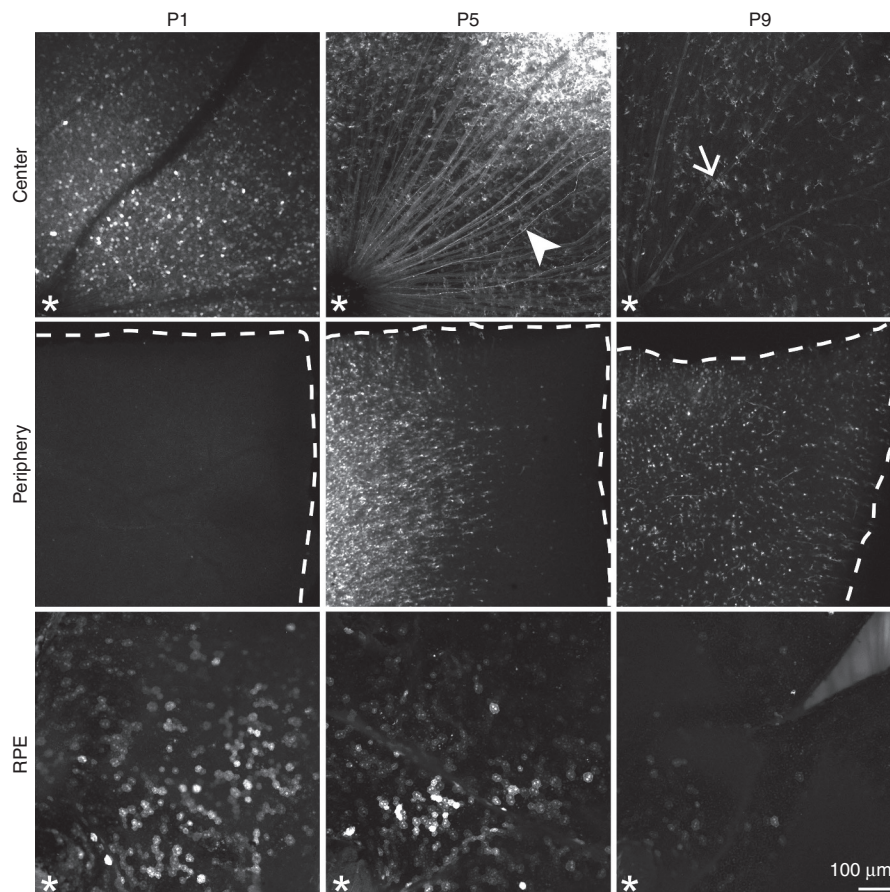


Figure 2 Characterization of retinal GFP expression in mice injected at various time points. Confocal images show the pattern of GFP expression in retinal whole mounts taken from adult mice injected at P1, P5 or P9 with AAV9-GFP. In the central retina (first row), mice injected at P1 had GFP-expressing cell bodies near the optic nerve head (ONH) (marked by asterisk). In contrast, mice injected at P5 had fewer GFP-positive cell bodies in the central retina, while axons traveling from peripheral ganglion cells are observed running toward the ONH (arrowhead). In mice injected at P9, GFP expression was observed in sparse retinal cells. The arrow indicates GFP expression in retinal blood vessels. P1-injected mice had no GFP expression in peripheral retina (second row), while P5 injected mice had GFP expression nearing the retinal edge (dashed line). P9-injected mice had sparse GFP expression in cells across the retina and up to the far edge. Images from RPE flatmounts (bottom row) showed that in P1-injected mice, there was strong GFP expression in RPE cells. In P5-injected mice, GFP expression was also present in RPE. In P9 mice, few RPE cells had strong GFP expression.

Different cell types are infected by injections performed at various ages

Different cell populations are born during specific windows in retinal development. In particular, ganglion cells, horizontal cells, amacrine cells, and photoreceptors are the first retinal cells to be born, whereas Müller glia and bipolar cells are born last.⁹ We therefore examined retinal cross sections to characterize the populations of cells transduced following systemic injections at varying time points (Figure 3). Groups of 5–7 mice were injected for each time point. Injections at P1 led to expression in all the cell types born earlier, while few Müller cells and bipolar cells were targeted. However, injections at P5 led to expression in large numbers of Müller cells (arrowhead) in addition to ganglion cells,

horizontal cells, amacrine cells, and photoreceptors. At P9, the majority of cells expressing GFP were Müller cells. Thus, the birth order of retinal cells directly impacts the cell types infected via systemic injection of AAV9 at specific time points.

The pattern of expression in neonatal brain is not affected by age at injection

AAV9 has also been shown to cross the blood–brain barrier to infect cells in the brain and spinal cord.¹⁰ Therefore, we also characterized AAV9 transduction in the brain following injection at specific time points in order to compare the effect of age on patterns of brain expression (Figure 4). Three mice were examined for each time point. In contrast to the retina, the pattern of

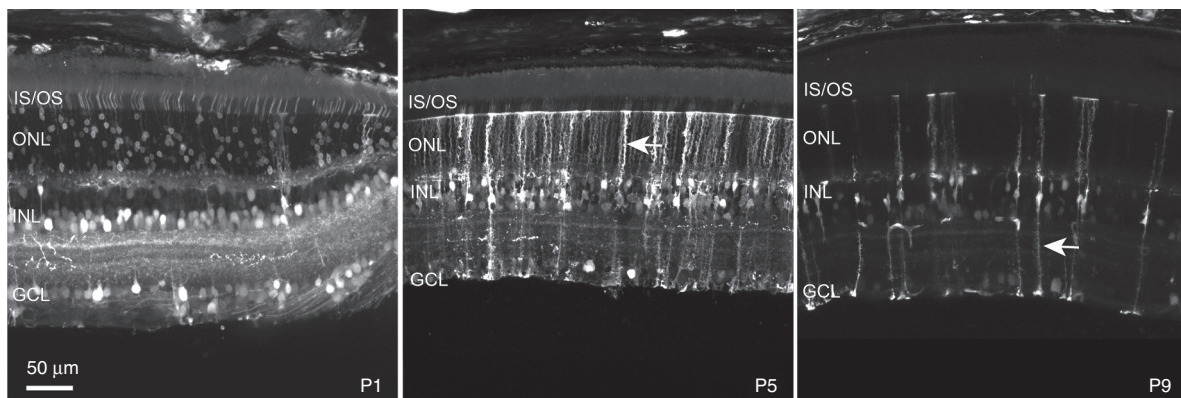


Figure 3 The retinal cell types targeted by systemic injections of AAV9 were determined by the age of injection. Confocal images of agarose-embedded retinal cross sections showed GFP expression in retinas from mice injected at P1, P5, or P9 and harvested 30 days after injection. In mice injected at P1, photoreceptors with cell bodies in the ONL, horizontal cells, amacrine cells, and ganglion cells strongly expressed GFP. Very few Müller cells and bipolar cells were infected. In mice injected at P5, in contrast, in addition to retinal neurons many Müller cells (identifiable by their radial morphology, and indicated by arrows) expressed GFP. In mice injected at P9, the majority of the cells expressing GFP were Müller glia.

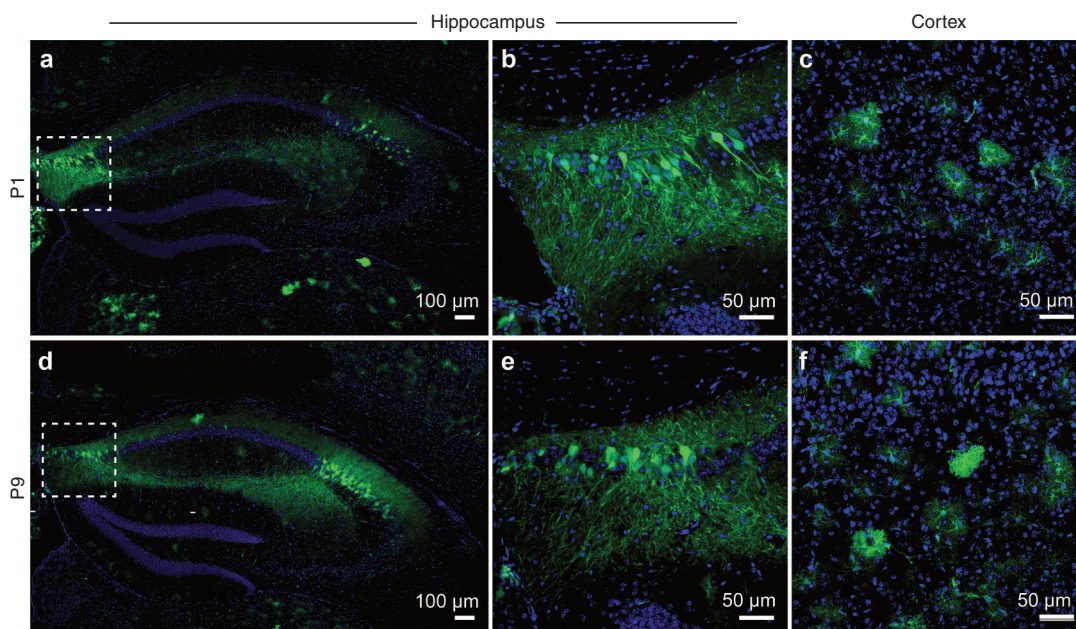


Figure 4 The expression pattern of systemically injected AAV9 in the neonatal brain was not affected by age at injection. Confocal images of brain sections showed similar patterns of GFP expression in mice injected at P1 and P9. At all time points tested, systemic injection of GFP resulted in GFP expression in hippocampal neurons (a,b,d,e). b and e showed high resolution images of the areas in the boxed portions of a and d. In the cortex, mice injected at P1 (c) and P9 (f) had GFP expression in cortical astrocytes, but few neurons. Blue is 4',6-diamidino-2-phenylindole (DAPI) labeling of cell nuclei.

expression in the brain was stable between P1 and P9. For instance, hippocampal neurons strongly expressed GFP in animals injected at P1, P3, P5, P7, and P9. Cerebellar neurons were also transduced (data not shown). Finally, the majority of cells in the cortex that expressed GFP were identifiable by their morphology as glia.

A larger area of the retina can be infected by sequential injections

Systemic delivery of AAV to the mouse retina holds great promise for proof-of-concept gene therapies and basic studies of retinal development. However, our results show that only a portion of the retina, determined by the age at injection, is transduced with a single injection, limiting the efficacy of this approach. Therefore, we tested whether larger portions of the retina could be targeted using sequential injections at two time points (Figure 5). Neonatal mice ($n = 5$) were injected at P1 with AAV9-mCherry and then again at P5 with AAV9-GFP. Using this method, up to 2/3 of the area of retina could be routinely transduced. Higher resolution images of the retinas (Figure 5b,c) showed nonoverlapping

populations of cells were transduced with P1 and P5 injections. Comparison of retinas injected at P1 alone, P5 alone or P1 and P5 showed that immune response, including the development of neutralizing antibodies against the vector capsid, did not appear to interfere with expression of the second vector, likely because of the short time interval between injections (Figure 5d).

Development and maturation of the retinal vasculature

Labeling of collagen-IV, an extracellular matrix component and part of the vascular basement membrane, was used to mark the growth and maturation of retinal blood vessels from P1 to P9 (Figure 6a). Three mice were imaged for each time point. One day after birth, a small growth of immature blood vessels was labeled surrounding the ONH. This plexus of blood vessels spread outward to the periphery until P7, when blood vessels reached to the extreme periphery of the retina. At P7, remodeling of the vascular network began to occur, and blood vessels grew in both area and complexity.

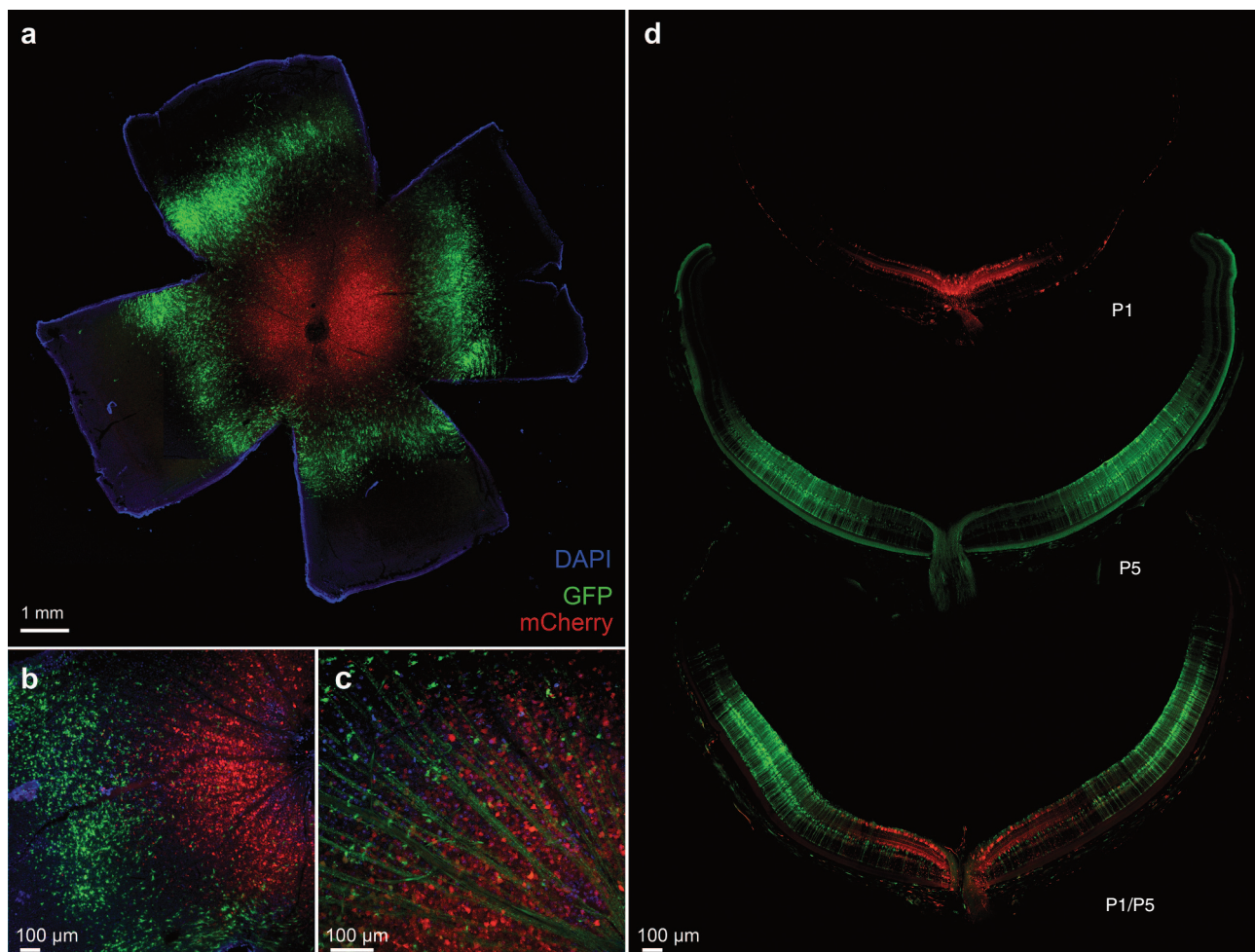


Figure 5 Sequential injections of AAV9-mCherry and AAV9-GFP cover an increased area of the retina. **(a)** Retinal whole mounts from mice injected at P1 with 10 μ L of AAV9-mCherry, and then again at P5 with 10 μ L of AAV9-GFP showed that a greater area of transgene expression was achieved by sequential injections. **(b)** 10 \times resolution image of mCherry and GFP expression showed nonoverlapping areas of infection. **(c)** 20 \times image taken near the optic nerve head showed axons from GFP-expressing cells in the periphery and the cell bodies of mCherry-expressing cells in the central retina. **(d)** Cross sections of retinas injected with AAV9-mCherry at P1 only (top) AAV9-GFP at P5 only (middle), or injected with the same number of particles of AAV9-mCherry at P1 and AAV9-GFP at P5 as were injected separately (bottom). Prior injection at P1 did not inhibit expression of P5 injections. Green is native GFP expression. Red is native mCherry expression. Blue is DAPI labeling of nuclei. DAPI, 4',6-diamidino-2-phenylindole.

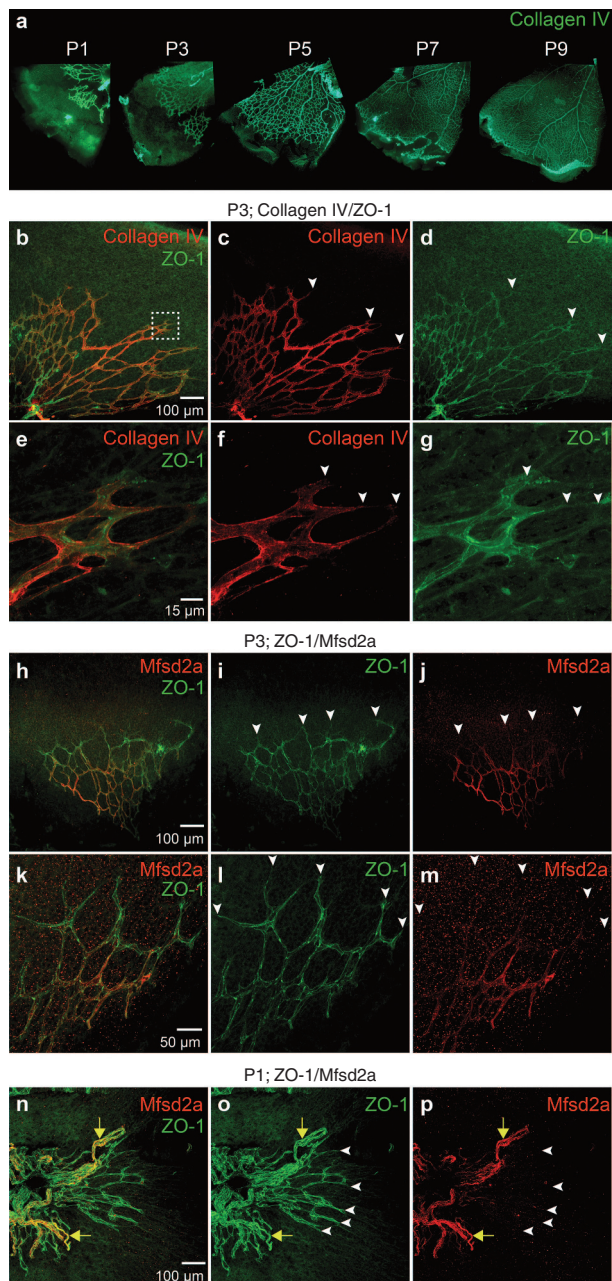


Figure 6 Maturation of the retinal vasculature in neonatal mice. Flatmounted retinas from neonatal mice stained with antibodies labeling collagen IV, ZO-1, or Mfsd2a showed the growth and maturation of retinal blood vessels. **(a)** Collagen IV labeling in one quadrant of a retinal flatmount showed the growth pattern of the retinal vasculature. One day after birth blood vessels radiating from the optic nerve head were limited to the central retina. Over time, the vascular network spread across the retina, until the entire area of the retina was covered. **(b–d)** Co-labeling of Collagen IV and ZO-1 in P3 retinas showed colocalization of blood vessels and tight junction proteins, up to the leading edge of blood vessel growth. **(e–g)** High resolution imaging of the boxed region in **(b)** showed the presence of ZO-1 at the tips of expanding blood vessels. **(h–m)** Co-labeling of Collagen IV and Mfsd2a showed that expression of Mfsd2a lagged behind the edge of blood vessel growth. A gradient of Mfsd2a expression was observed, with labeling seen most strongly at the center of the retina and lacking at the outer edges. In P1 retina **(n–p)**, Mfsd2a labeling showed strong expression in receding hyaloid blood vessels (yellow arrows), while labeling was not seen in newly developing retinal blood vessels. Arrowheads indicate the edge of blood vessel growth.

Tight junctions comprise a major component of the blood–brain and blood–retina barriers. We therefore tested whether the AAV permeability of developing retinal blood vessels at leading edge of vascular growth might be due to an underdevelopment of the tight junction architecture. Immunolabeling of ZO-1 in P3 retinas (**Figure 6b–g**), however, showed that the pattern of expression of ZO-1 closely corresponded to labeling of collagen IV, including at the edge of blood vessel growth ($n = 5$). This suggests that a delay in the expression of tight junctions does not contribute to permeability of retinal blood vessels.

Recently, Mfsd2a, a transporter for the essential omega-3 fatty acid docosahexaenoic acid,¹¹ has been identified as a marker for maturity of the blood–brain barrier and necessary for its integrity.¹² We therefore labeled Mfsd2a in the developing retina. Labeling of neonatal retinas showed that a developmental wave of Mfsd2a expression lags behind the growth of retinal blood vessels, indicating that the blood–retina barrier matures from the center outward (**Figure 6h–p**). In P3 retinas, a gradient of Mfsd2a labeling was observed, with stronger expression in the center of the retina, and with a lack of labeling at the edge of blood vessel growth (**Figure 6h–m**). In P1 retinas, while regressing hyaloid vessels were labeled strongly for Mfsd2a, developing retinal vasculature lacked Mfsd2a labeling (**Figure 6n–p**). Four mice were imaged for each time point examined.

DISCUSSION

While systemic injections of AAV9 for the treatment of retinal and neurological disease have not yet been proven in a clinical setting, they may offer advantages for the treatment of disorders requiring early intervention, conditions in which intraocular injections are not possible, such as retinoblastoma, or diseases affecting multiple organs. Some of the most significant problems include off-target vector tropism, low efficiency of expression, and the presence of preexisting neutralizing antibodies in adults. However, studies in rodents, dogs, cats, and primates have shown the feasibility of systemic AAV delivery.

Systemic injections are noninvasive to the eye, and are thus advantageous for the delivery of transgenes to the retina in mice at early time points. The window for treatment in many mouse models of retinal degeneration is small, since they progress quickly. For example, in the widely studied *rd1* mouse, photoreceptors are lost by P8.¹³ Intraocular injections at such an early time point are damaging to the developing eye structure and can lead to microphthalmia. In contrast, systemic injections avoid damage to the eye and may represent a preferable alternative as a noninvasive approach to treat the underlying cause of degeneration before cell loss occurs.

In addition, systemic injections may have potential application to retinal diseases for which intraocular injections would represent additional risk. For example, high intraocular pressure in glaucoma is thought to play a role in the degeneration of retinal ganglion cells, and local injection of a gene therapy vector may increase pressure and cause additional damage. Additionally, the wet and dry forms of age-related macular degeneration are often associated with abnormal choroidal neovascularization and increased risk of retinal detachment, and therefore these diseases might benefit from a systemic approach.

Syndromes affecting multiple tissues might also be treated with a single systemic injection. Lysosomal storage diseases such as mucopolysaccharidoses, Bardet–Biedl syndrome, Usher Syndrome, or neurodegenerative disorders affecting the brain, retina, and/or spinal cord may be targets for systemic treatments.

We show here that systemic delivery of AAV9 has potential for the delivery of gene therapies to the retina, and that the development of the retinal vasculature determines the pattern of expression of AAV9. In mice, development of the retinal vasculature occurs after birth, but is analogous to the development of retinal vasculature in humans *in utero*. In humans, vasculogenesis begins around the optic disc at around 14–15 weeks gestation, and reaches the periphery by 37–40 weeks gestation.⁸ These studies may therefore have implications for the feasibility of and may inform approaches to an *in utero* systemic treatment to treat retinal disease. *In utero* treatments may allow for the earliest possible intervention, in cases where the mutation is already known at this stage, and they have been suggested to be an approach to avoid immune response as a result of prior AAV exposure, since an estimated 33.5% of the human population has preexisting seropositivity to AAV9.¹⁴

However, our results show that only a limited area of the retina, corresponding to the leading edge of vasculogenesis, can be transduced with a single injection. Through timing of the injection, specific populations of cells can be targeted, with the region and cell type varying depending on the age at injection. Sequential injections can be made during retinal vasculature development, resulting in concentric rings of expression and increasing the area transduced. Up to 2/3 of the retina can be covered by combining two sequential injections.

In mice, intravitreal or intramuscular injections of AAV lead to the production of neutralizing antibodies, peaking 2 months after treatment.¹⁵ Here we show that injections made at P1 do not inhibit expression of injections made at P5, indicating that the immune response does not develop rapidly enough to limit expression from sequential systemic injections performed in this time frame.

We also characterized the maturation of retinal vasculature in mice, in order to understand the mechanism by which AAV9 crosses the vasculature to infect the retina. Our results show that ZO-1 is present at the far peripheral edge of vasculogenesis, suggesting that lack of tight junctions does not underlie the ability of AAV9 to cross the vasculature into retinal neurons. In contrast, Mfsd2a labeling was observed in a gradient, expressing most strongly in the central area of the retina, and lacking in the edge of blood vessel growth, the area corresponding to the area of AAV9-GFP expression. Recently, Mfsd2a was shown to be necessary for the integrity of the blood–brain barrier, and onset of Mfsd2a expression corresponded to a decrease in transcytosis, while mice lacking Mfsd2a protein had dramatic increase of transcytosis and a breakdown of the blood–brain barrier integrity. Although the exact mechanism by which AAV9 crosses the blood–brain and blood–retina barriers is not known, AAV has been suggested to cross epithelial barriers through transcytosis.^{16–18} Our results indicate that AAV9 may cross the developing blood–retina barrier through transcytosis, and that onset of

Mfsd2a expression limits transduction of the retina through a suppression of transcytosis.

In summary, these studies further raise the possibility that AAV may be used as a tool to study retinal development and to target particular regions of the retina, by timing the injection to target a particular region of the retina. Additionally, systemic AAV9 injections could be used to investigate breakdown of blood–brain barrier integrity, especially any breakdown resulting from decreased suppression of transcytosis. Finally, these studies further advance the possibility of harnessing systemic AAV administration to treat central nervous system and retinal disease.

MATERIALS AND METHODS

Animals. All procedures were performed in accordance with the Association for Research in Vision and Ophthalmology statement for the Use of Animals in Ophthalmic and Vision Research, and were approved by the University of California Animal Care and Use Committee. C57BL/6J mice from Jackson Laboratories were used for all experiments.

AAV vector production. AAV9 vectors with two tyrosine-to-phenylalanine mutations carrying GFP or mCherry were produced by the plasmid co-transfection method.¹⁹ AAV92YF was used for all of the experiments performed. Recombinant AAV was purified by iodixanol gradient ultracentrifugation followed by a buffer exchange and concentration with Amicon Ultra-15 Centrifugal Filter Units in phosphate-buffered saline (PBS). Titers were determined by quantitative polymerase chain reaction relative to a standard curve.²⁰

Intravenous injections. Pups were immobilized, and an operating microscope was used to visualize the tail vein. A total of 5×10^{11} DNase-resistant viral particles were injected in a 10 μ l volume in mice from P1–P5. For mice injected at P7–P9, 1×10^{12} DNase-resistant viral particles were injected in a 20 μ l volume. A correct injection was verified by observed blanching of the vein. After the injection, pups were allowed to recover for several minutes on a heating pad before being returned to their cages.

Agarose embedding. Eyecups were freshly dissected and immediately placed in 10% formalin overnight. Eyecups were then rinsed in PBS and embedded in 5% agarose. Using a vibratome, 150 μ m transverse sections were cut, and the sections were postfixed in 4% paraformaldehyde for 10 minutes, then floated in PBS. After washing, sections were mounted with 4',6-diamidino-2-phenylindole (DAPI)-containing media for confocal imaging. All GFP imaging was performed without amplification of native GFP expression (LSM710, Carl Zeiss, Jena, Germany).

Immunolabeling. Retinas were freshly dissected and fixed in 4% paraformaldehyde overnight. Retinas were rinsed in PBS, and after blocking in 1% bovine serum albumin, 0.5% Triton X-100, and 2% normal donkey serum for 2–3 hours at room temperature, whole mounts were incubated in primary antibody overnight at 4 °C. After washing in PBS, secondary antibodies were applied at room temperature for 1 hour. Retinas were again washed, and relief cuts were made. Retinas were then mounted for confocal microscopy. For Mfsd2a labeling, retinas were permeabilized in 0.3% PBS-Triton-X for 3 hours. Antibody was diluted 1:250 in 10% NGS in 0.1% PBS-Triton-X and incubated for 24 hours at 4 °C. Antibodies were as follows: rabbit anti-Collagen IV, (Abcam, 1:250); mouse anti-ZO-1 (Life technologies, 1:100); rabbit anti-Mfsd2a (gift of Professor David Silver, 1:250).

Brain sectioning. Mouse brains were extracted after ketamine euthanasia and intracardiac perfusion with 4% paraformaldehyde. After soaking in 4% paraformaldehyde at 4 °C for at least 24 hours, the fixed brains were transferred to PBS for 24 hours. For cryoprotection, the brains were incubated in a sucrose-PBS solution until the tissue sank, first at 15% sucrose and then 30% sucrose. Whole brains were then embedded in Tissue Freezing Medium

(Triangle Biomedical Sciences, Durham, NC) and coronal sections 40 μm or 100 μm in thickness were collected at $-23\text{ }^{\circ}\text{C}$ in a cryostat-microtome.

ACKNOWLEDGMENTS

We thank Meike Visel for advice and assistance with viral vector packaging. We thank David L. Silver, Duke-NUS Graduate Medical School, Singapore, for the Mfsd2a antibody. The authors declare that the research was conducted in the absence of any commercial or financial relationships that could be construed as a potential conflict of interest. This work was supported by funding from the NIH, the FFB, and a Ruth L. Kirschstein National Research Service Award.

REFERENCES

- Bostick, B, Ghosh, A, Yue, Y, Long, C and Duan, D (2007). Systemic AAV-9 transduction in mice is influenced by animal age but not by the route of administration. *Gene Ther* **14**: 1605–1609.
- Rahim, AA, Wong, AM, Hofer, K, Buckley, SM, Mattar, CN, Cheng, SH *et al.* (2011). Intravenous administration of AAV2/9 to the fetal and neonatal mouse leads to differential targeting of CNS cell types and extensive transduction of the nervous system. *FASEB J* **25**: 3505–3518.
- Dalkara, D, Byrne, LC, Lee, T, Hoffmann, NV, Schaffer, DV and Flannery, JG (2012). Enhanced gene delivery to the neonatal retina through systemic administration of tyrosine-mutated AAV9. *Gene Ther* **19**: 176–181.
- Joussemet, B, Belbellaa, B, Mendes-Madeira, A, Bucher, T, Briot-Nivard, D, Dubreil, L *et al.* (2011). Neonatal systemic delivery of scAAV9 in rodents and large animals results in gene transfer to RPE cells in the retina. *Exp Eye Res* **93**: 491–502.
- Mattar, CN, Waddington, SN, Biswas, A, Johana, N, Ng, XW, Fisk, AS *et al.* (2013). Systemic delivery of scAAV9 in fetal macaques facilitates neuronal transduction of the central and peripheral nervous systems. *Gene Ther* **20**: 69–83.
- Petrs-Silva, H, Dinculescu, A, Li, Q, Min, SH, Chiodo, V, Pang, JJ *et al.* (2009). High-efficiency transduction of the mouse retina by tyrosine-mutant AAV serotype vectors. *Mol Ther* **17**: 463–471.
- Fruttiger, M (2007). Development of the retinal vasculature. *Angiogenesis* **10**: 77–88.
- Provis, JM (2001). Development of the primate retinal vasculature. *Prog Retin Eye Res* **20**: 799–821.
- Cepko, CL, Austin, CP, Yang, X, Alexiades, M and Ezzeddine, D (1996). Cell fate determination in the vertebrate retina. *Proc Natl Acad Sci U S A* **93**: 589–595.
- Foust, KD, Nurre, E, Montgomery, CL, Hernandez, A, Chan, CM and Kaspar, BK (2009). Intravascular AAV9 preferentially targets neonatal neurons and adult astrocytes. *Nat Biotechnol* **27**: 59–65.
- Nguyen, LN, Ma, D, Shui, G, Wong, P, Cazenave-Gassiot, A, Zhang, X *et al.* (2014). Mfsd2a is a transporter for the essential omega-3 fatty acid docosahexaenoic acid. *Nature* **509**: 503–506.
- Ben-Zvi, A, Lacoste, B, Kur, E, Andreone, BJ, Mayshar, Y, Yan, H *et al.* (2014). Mfsd2a is critical for the formation and function of the blood-brain barrier. *Nature* **509**: 507–511.
- Bowes, C, Li, T, Danciger, M, Baxter, LC, Applebury, ML and Farber, DB (1990). Retinal degeneration in the rd mouse is caused by a defect in the beta subunit of rod cGMP-phosphodiesterase. *Nature* **347**: 677–680.
- Boutin, S, Monteilhet, V, Veron, P, Leborgne, C, Benveniste, O, Montus, MF *et al.* (2010). Prevalence of serum IgG and neutralizing factors against adeno-associated virus (AAV) types 1, 2, 5, 6, 8, and 9 in the healthy population: implications for gene therapy using AAV vectors. *Hum Gene Ther* **21**: 704–712.
- Li, Q, Miller, R, Han, PY, Pang, J, Dinculescu, A, Chiodo, V *et al.* (2008). Intraocular route of AAV2 vector administration defines humoral immune response and therapeutic potential. *Mol Vis* **14**: 1760–1769.
- Shen, S, Bryant, KD, Brown, SM, Randell, SH and Asokan, A (2011). Terminal N-linked galactose is the primary receptor for adeno-associated virus 9. *J Biol Chem* **286**: 13532–13540.
- Bell, CL, Vandenberghe, LH, Bell, P, Limberis, MP, Gao, GP, Van Vliet, K *et al.* (2011). The AAV9 receptor and its modification to improve *in vivo* lung gene transfer in mice. *J Clin Invest* **121**: 2427–2435.
- Di Pasquale, G and Chiorini, JA (2006). AAV transcytosis through barrier epithelia and endothelium. *Mol Ther* **13**: 506–516.
- Grieger, JC, Choi, VW and Samulski, RJ (2006). Production and characterization of adeno-associated viral vectors. *Nat Protoc* **1**: 1412–1428.
- Aurnhammer, C, Haase, M, Muether, N, Hausl, M, Rauschhuber, C, Huber, I *et al.* (2012). Universal real-time PCR for the detection and quantification of adeno-associated virus serotype 2-derived inverted terminal repeat sequences. *Hum Gene Ther Methods* **23**: 18–28.